

HeartLogic™
Heart Failure Diagnostic

SOME TECHNOLOGY IS GAME CHANGING.

THIS IS CAREER DEFINING.

Lead the way with HeartLogic™ from Boston Scientific. The first and only FDA-approved heart failure alert validated to have: high sensitivity, the ability to provide weeks of advanced notice, and low alert burden for detecting worsening heart failure.¹ This is your time. It's your move.

Only available in the Boston Scientific Resonate™ family of CRT-Ds and ICDs.

LEARN MORE ABOUT HEARTLOGIC

Rx only.

¹ Boehmer JP, Hariharan R, Deveochi FG, et al. A Multisensor algorithm predicts heart failure events in patients with implanted devices: results from the MultiSENSE study. JACC Heart Fail. 2017 Mar;5(3):216-25. CRM-572611-AA

Measurements of Electrophysiological Effects of Components of Acute Ischemia in Langendorff-Perfused Rat Hearts Using Voltage-Sensitive Dye Mapping

ANDERS NYGREN, PH.D.,*†, ISTVÁN BACZKÓ, M.D., PH.D.,* and WAYNE R. GILES, PH.D.*†

From the *Department of Physiology and Biophysics, University of Calgary, Calgary, Alberta, Canada; †Whitaker Institute of Biomedical Engineering University of California, San Diego, La Jolla, California, USA; and ‡ Centre for Bioengineering Research and Education, Department of Computer and Electrical Engineering, University of Calgary, Calgary, Alberta, Canada

Optical Mapping of Components of Ischemia in Rat Heart. *Introduction:* This study was carried out to evaluate optical mapping in the presence of cytochalasin-D as a method for measuring electrophysiological responses in general, and in particular the responses to acute ischemia in the Langendorff-perfused rat heart. Cytochalasin-D is commonly used to reduce contraction for the purpose of suppressing motion artifacts in voltage-sensitive dye recordings of cardiac membrane potential.

Methods and Results: Observations using optical mapping were complemented by recordings of the surface electrogram to provide information independent of the optical measurements. Perfusion of Langendorff-perfused rat hearts with 3 μM cytochalasin-D resulted in a 24% prolongation of the QT interval of surface electrograms indicating that cytochalasin-D prolongs the rat ventricular action potential. Individual components of the electrophysiological response to acute ischemia were globally induced as follows: (1) opening of K_{ATP} channels was induced by perfusion of 2 μM P-1075, (2) accumulation of extracellular K^+ was simulated by increasing perfusate $[\text{K}^+]$ to 12 mM, and (3) acidosis was simulated by reducing perfusate pH to 6.5. The responses to these interventions could be reliably documented using optical recordings, as well as from surface electrograms. Whole-cell patch clamp measurements on isolated rat ventricular myocytes indicate that cytochalasin-D produces an approximately 2.5-fold increase in P-1075-induced $\text{I}_{\text{K,ATP}}$.

Conclusion: These results provide the necessary background information for interpreting electrophysiological measurements during acute ischemia in the presence of cytochalasin-D. (*J Cardiovasc Electrophysiol*, Vol. 17, pp. S113-S123, Suppl. 1, May 2006)

ischemia, fluorescent dye imaging, optical mapping, cytochalasin-D

Introduction

Optical mapping techniques based on voltage-sensitive dyes are frequently used to study the dynamics of cardiac arrhythmias.¹ These methods have many advantages, including high spatial and temporal resolution, direct recording of transmembrane (as opposed to extracellular) potential, and the absence of artifacts caused by electrical stimulation.¹ A large number of studies of cardiac arrhythmias using optical mapping have been published, including several that specifically address arrhythmias arising in the context of ischemia.²⁻⁸ One of the most significant limitations of optical mapping techniques to date is the presence of “motion artifacts” (artificial signals caused by the contraction of the heart muscle). Since these motion artifacts coincide with the repolarization phase of the action potential, they must usually be suppressed by using pharmacological agents that reduce contraction amplitude. There are two such “motion block-

ers” currently in frequent use: 2,3-butanedione monoxime (BDM) and cytochalasin-D (cyto-D). Unfortunately, both of these motion blockers may have significant side effects. BDM is known to inhibit many ionic currents at concentrations required to reduce motion artifacts. As a result, BDM alters the action potential duration (APD) in most species. The exact effect on the APD varies depending on the roles of affected ionic currents in the cardiac action potential in different species. For example, BDM shortens the APD in sheep and guinea pig,⁹ but prolongs the APD in the mouse.¹⁰ BDM has also been shown to enhance shock-induced arrhythmias,¹¹ and to provide a protective effect during reperfusion after ischemia.¹² As a result of these side effects, and in particular the effects directly related to ischemia, BDM may not be suitable as a motion blocker for ischemia studies.

Cyto-D is a commonly used pharmacological tool to study the actin cytoskeleton. The primary effect of cyto-D on contractility of cardiac myocytes is most likely due to a decrease in myofilament (sarcomeric actin) sensitivity to Ca^{2+} rather than cyto-D effects on the actin cytoskeleton.¹³ However, disruption of the cytoskeleton using cyto-D has been shown to have a number of effects on ion channels and intracellular signaling pathways.¹³ Of particular note in the context of ischemia is the effect on the ATP-sensitive K^+ channel, $\text{I}_{\text{K,ATP}}$. Disruption of the actin cytoskeleton is known to enhance K_{ATP} channel rundown,¹⁴ enhance K_{ATP} channel opening,¹⁵ and reduce inhibition of K_{ATP} channels by sulfonyleurea drugs.^{16,17} The use of cyto-D as a motion blocker can thus potentially alter the function of K_{ATP} channel, as well as the

This study was supported by grants from the Canadian Institutes for Health Research (CIHR), the Heart & Stroke Foundation of Canada (HSFC), and the Alberta Heritage Foundation for Medical Research (AHFMR). Dr. Nygren held a HSFC Research Fellowship during the initial stages of this project.

Address for correspondence: Wayne R. Giles, Ph.D., Whitaker Institute of Biomedical Engineering, PFBG 384, University of California, San Diego, 9500 Gilman Dr, La Jolla, CA 92093-0412. Fax: +1-858-534-4535; E-mail: wgiles@bioeng.ucsd.edu

doi: 10.1111/j.1540-8167.2006.00392.x

baseline APD. Compared to BDM, cyto-D has been reported to have either no or less pronounced effects on APD in canine, rabbit, and swine ventricles.¹⁸⁻²¹ However, in the mouse ventricle cyto-D has been shown to significantly prolong the APD.^{10,22} In isolated rat ventricular cells, Yang et al.²³ reported that cyto-D had no effect on transient outward current or APD, except in hypertrophied myocytes. At present, there are no results from whole rat hearts available in the literature.

The isolated Langendorff-perfused rat heart has become a commonly used model for studying arrhythmias, and in particular ischemia-induced ventricular fibrillation (VF).^{24,25} Among the factors contributing to the use of this experimental model is the fact that the rat heart is known to lack effective coronary collaterals, which results in reproducible ischemic zones in response to coronary ligation.²⁴ In addition, rats are relatively inexpensive and readily available, making them an attractive preparation for many applications in cardiovascular electrophysiology. The availability of the rat genome is likely to generate increased interest in the rat as an experimental model.²⁶ We have previously demonstrated the feasibility of optical mapping in the Langendorff-perfused rat heart.²⁷ However, despite the popularity of the rat heart as an experimental model in the context of ischemia, there have been no reports of optical mapping studies performed in the Langendorff-perfused rat heart in this context. One obstacle to such studies is the presence of motion artifacts as discussed above and thus the need to use motion blockers so that repolarization and APD can be reliably measured. This study was carried out to evaluate optical mapping in the presence of cyto-D as a method for measuring electrophysiological responses to acute ischemia in the Langendorff-perfused rat heart. Three primary effects of acute ischemia, namely, (1) opening of K_{ATP} channels, (2) elevation of extracellular $[K^+]$, and (3) acidosis²⁸ were induced separately so that their individual electrophysiological effects could be measured. Observations using optical mapping are complemented by recordings of the surface electrogram to provide information independent of the optical measurements.

Methods

Isolation of Single Rat Ventricular Myocytes

Adult male Sprague-Dawley rats were euthanized with pentobarbital (150 mg/kg, i.p.) according to the University of Calgary Animal Care Committee and the Canadian Council on Animal Care (CCAC) Guidelines. The hearts were then removed and ventricular myocytes were obtained by enzymatic dissociation using the standard protocols described previously.^{29,30} After one hour, cells were placed on cover slips for observation at 200 \times with an inverted microscope and were allowed to adhere to the bottom of the recording chamber for five minutes followed by superfusion with control solution containing (in mM) NaCl 140, KCl 5.4, HEPES 10, CaCl₂ 1.0, MgCl₂ 1.4, and glucose 10 (pH = 7.4).

Whole-Cell Patch Clamp Measurements

Two inwardly rectifying K^+ currents, I_{K1} and $I_{K,ATP}$, were recorded in the whole-cell configuration of the patch clamp technique at room temperature ($22 \pm 1^\circ\text{C}$). Patch pipettes were pulled using borosilicate glass (G85150T, Warner In-

strument Corp., Salt Lake City, UT, USA) to yield pipettes with a resistance of 2–4 M Ω when filled with pipette solution. Recorded membrane potentials were corrected by -10 mV to compensate for junction potentials between bath and pipette solutions. Pipettes were back-filled with a solution containing the following (in mM): K-aspartate 120, KCl 20, HEPES 10, NaCl 8, MgCl₂ 1.4, EGTA 10, CaCl₂ 1, K₂ATP 2, glucose 10. The pH of the solution was adjusted to 7.2 with KOH. Once a G Ω seal was formed, access to the cell was achieved by rupturing the membrane under the pipette by applying gentle suction; a series resistance of <10 M Ω was deemed acceptable. Pipette series resistance compensation was applied to reduce it by 80–90%. Membrane current recordings were made using an Axopatch 200B patch clamp amplifier controlled with Clampex 8.0 software (Axon Instruments, Foster City, CA, USA) for data acquisition and analysis. Data were sampled at 1 kHz, digitized (Digidata 1320A, Axon Instruments) and stored on computer. Cells were voltage clamped to -80 mV, and then I_{K1} I-V relations were determined by applying 300-msec long voltage ramps from $+40$ mV to -120 mV. I_{K1} was the difference current obtained by subtraction of current remaining after exposure of the cell to 200 μM BaCl₂ containing solution from the recorded current in the corresponding control solution.³¹ A solution containing 50 μM P-1075 was used to induce $I_{K,ATP}$; for the inhibition of $I_{K,ATP}$, 10 μM HMR 1098 was added to the solution. All measured whole-cell currents were normalized to cell capacitance.

Langendorff-Perfused Rat Hearts

All experiments followed the guidelines of the University of Calgary Animal Care Committee and the Canadian Council for Animal Care. Rat hearts were isolated using a procedure described previously.²⁷ Briefly, male Sprague-Dawley rats (250–300 grams) were injected with 300 U of heparin (i.p.) 15 minutes before the heart was isolated. The animals were anaesthetized with pentobarbital and sacrificed by cervical dislocation, after which the heart was immediately excised and placed in ice-cold Krebs-Henseleit solution. The aorta was cannulated and perfusion with Krebs-Henseleit solution (37°C) was started at a constant flow rate of approximately 13 mL/min. The Krebs-Henseleit buffer consisted of (in mM) NaCl 118.0, KCl 4.7, KH₂PO₄ 1.2, MgSO₄ 1.2, CaCl₂ 2.0, NaHCO₃ 25.0, and glucose 11.1, bubbled with 95% O₂/5% CO₂ in a 37°C water bath for a pH of 7.4. All solutions were filtered using a 5- μm pore membrane filter (Millipore, Bedford, MA, USA). Perfusion pressure and temperature of the perfusate and the preparation were monitored as described previously.²⁷ After a 30-minute stabilization period, the solution was switched to one containing 1 μM di-4-ANEPPS (Molecular Probes, Portland, OR, USA) for a period of five minutes. Di-4-ANEPPS was prepared as 10 mM stock solution in DMSO (stored frozen) and added to the standard Krebs-Henseleit solution (0.01% DMSO in the final solution). To reduce the influence of motion artifacts on our recordings, the heart was positioned in the chamber by adjustable supports and mechanically restrained for short periods of time (≈ 10 seconds) during each recording as described previously.²⁷ Cyto-D (Sigma-Aldrich, Oakville, ON, Canada) at a concentration of 3 μM ,²¹ was used as a pharmacological motion blocker where noted.

Recording of Surface Electrograms

Electrodes consisting of loops of Ag wire coated with AgCl were sutured onto the epicardial surface for recording of surface electrograms. In all recordings used for interval analysis, three electrodes were attached to the heart (at the left ventricular apex, left ventricular base, and right ventricular base), providing three differential signals (“leads”). Our intent with this three-lead configuration was to provide an approximation of the vectors recorded by the standard three-lead electrocardiogram, although we acknowledge that these near-field recordings cannot be directly compared to body surface recordings. Electrograms were recorded with an AC-coupled differential amplifier (Model 1700, A-M Systems, Carlsborg, WA, USA) with a high pass cutoff of 0.1 Hz. Signals were low pass filtered at 500 Hz and acquired at the same sampling rate as the optical mapping data (950 Hz). Electrogram signals shown in this article are signal averaged over 20 seconds of recordings. Averaged signals were analyzed manually to determine relevant intervals, using custom software written in interactive data language (IDL) (Research Systems, Boulder, CO, USA).

Imaging System

The imaging system has been described in detail elsewhere.²⁷ Briefly, illumination was provided by a 250 W Quartz Tungsten Halogen (QTH) light source (Oriel Instruments, Stratford, CT, USA), and filtered with a 500 ± 25 nm interference bandpass filter (Omega Optical, Brattleboro, VT, USA). The resulting light was directed onto the preparation using a dichroic mirror (Omega Optical). The light emitted from the preparation passed through the dichroic mirror and a long pass (>590 nm) Schott glass filter (Melles Griot Canada, Ottawa, ON, Canada) before reaching the camera. The camera was a Dalsa CA-D1-0128T camera (Dalsa, Waterloo, ON, Canada), used in a binning mode, resulting in 60×60 pixels acquired with 12-bit resolution at 950 frames/sec. Equipped with a 25 mm focal length lens (CF25L, Fujinon, Wayne, NJ, USA) and a 3 mm spacer, it produced a 15×15 mm field of view ($250 \times 250 \mu\text{m}/\text{pixel}$). Electrocardiogram (ECG) data, bath temperature, pressure, and the trigger signal for the stimulator were all recorded using a National Instruments PCI-7030/6030E real-time data acquisition board (National Instruments, Austin, TX, USA). The ECG and stimulus data acquisition were synchronized to the camera, and this allowed these signals to be used as a reference for signal averaging.

Image Data Processing

Data were processed offline using software developed in the IDL development environment (Research Systems), with external routines written in C++ (Visual C++, Microsoft, Redmond, WA, USA) for the most computationally demanding tasks. The data recorded for each individual pixel were processed as follows: (1) the background fluorescence level was subtracted from the signal, (2) any linear trend in the data was removed, and (3) the sign of the data was changed so that a depolarization corresponded to a positive change in the signal. Areas of the field of view not covering the preparation were manually masked and excluded from further analysis. The activation time for each pixel was detected as the time of maximum rate of rise of the fluorescence signal.³² Activation maps were computed for individual cycles with activation

times referenced to the stimulus pulse (paced rhythms) or the R (or S) wave of the ECG (sinus rhythm). Signal-averaged activation maps were then computed by averaging the activation times for individual pixels over all cycles. The activation maps used in this article are signal averaged over five seconds of recording (20–25 cycles).

Repolarization times were detected as the time of crossing a level corresponding to 80% repolarization. The detection was based on low pass filtered (11-point moving average smoothing) and signal-averaged data, to avoid spurious detections due to remaining noise. Action potentials at individual pixel locations affected by either remaining motion artifact or unusually low signal-to-noise ratio were excluded based on the following heuristic criteria, applied to the signal-averaged but unfiltered signal: (1) the signal must remain below 15% of maximum amplitude until 15 msec before the detected activation (max rate of rise) time (to exclude signals with unstable baseline and/or large noise), (2) the signal must reach above 90% of maximum amplitude within 20 msec after the activation time (to exclude signals with very slow upstrokes), and (3) the signal must return (and remain) below 15% of maximum amplitude by 100 msec after the activation time (to exclude signals with unstable baseline, large noise, or unreasonably long apparent APDs due to motion artifacts). APDs were then computed as the intervals between the activation time and the repolarization time detected for each pixel.

Statistical Analysis

Data are presented as mean \pm SEM. Hypothesis testing was carried out using unpaired or paired *t*-tests as appropriate in cases with only two groups, and analysis of variance (ANOVA) or repeated measures ANOVA followed by the Holm *t*-test for three or more groups. A *P* value of less than 0.05 was considered statistically significant.

Results

Effect of Cyto-D on I_{K1} and $I_{K,ATP}$

The K^+ channel opener P-1075³³ and the sulfonylurea HMR 1098^{34,35} were used in this study to activate and block the ATP-sensitive K^+ current, $I_{K,ATP}$. Whole-cell patch clamp studies on isolated rat ventricular myocytes were used to assess the effect of $3 \mu\text{M}$ cyto-D on the efficacy of these agents. Whole-cell current at a fixed membrane potential (0 mV) was used as a measure of the current activated by P-1075. Figure 1A shows the amplitude of this current before and after the application of $2 \mu\text{M}$ P-1075, under control conditions (no cyto-D present) and in the presence of $3 \mu\text{M}$ cyto-D. On average, the P-1075-induced current was approximately 2.5 times larger in the presence of $3 \mu\text{M}$ P-1075, suggesting that cyto-D can facilitate activation of $I_{K,ATP}$ by P-1075. There was no significant difference (control vs $3 \mu\text{M}$ cyto-D) in the size of the current recorded at 0 mV prior to the application of P-1075. The possible effects of cyto-D on the efficacy of HMR 1098 as a K_{ATP} channel blocker were also assessed. After the P-1075-induced current had been measured, $10 \mu\text{M}$ HMR 1098 was added to the superfusate (in the continued presence of $2 \mu\text{M}$ P-1075) and the current at 0 mV was measured again. Figure 1B shows a summary of these observations, expressed as the percentage of the current activated by $2 \mu\text{M}$ P-1075 that was subsequently blocked by the application of $10 \mu\text{M}$ HMR 1098. No significant

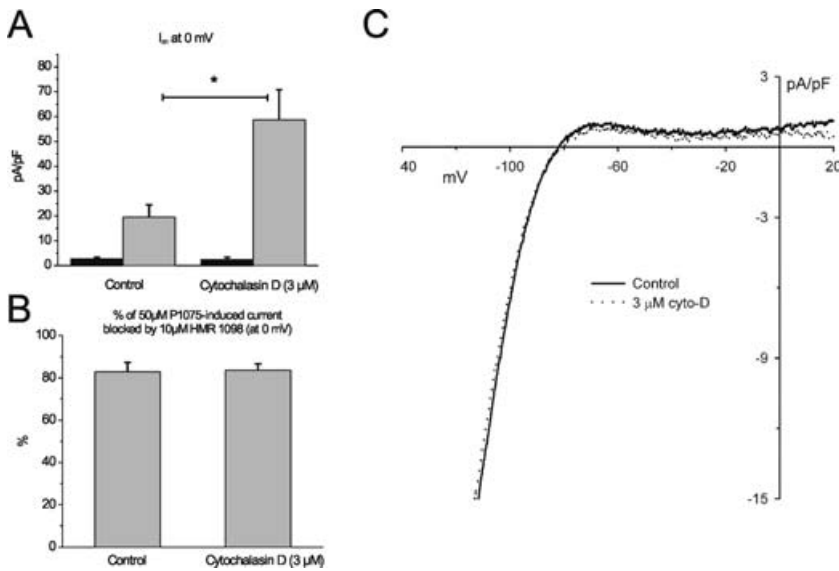


Figure 1. Effect of the motion blocker cyto-D on the properties of $I_{K,ATP}$ and I_{K1} currents. A: Current ($I_{K,ATP}$) at 0 mV membrane potential induced by 50 μ M P-1075 in the absence (control) and presence of 3 μ M cyto-D. B: Percentage block of P-1075-induced current at 0 mV membrane potential by 10 μ M HMR 1098. C: Current-voltage relationship for the inwardly rectifying current I_{K1} in the absence (control) and presence of 3 μ M cyto-D. I_{K1} current was measured as the Ba^{2+} -sensitive component of whole-cell current (see text).

effect of 3 μ M cyto-D on the efficacy of HMR 1098 was observed.

The possibility that 3 μ M cyto-D affects the inwardly rectifying K^+ current, I_{K1} , was also evaluated using whole-cell patch clamp measurements. I_{K1} was measured as the difference in whole-cell current before and after the application of 200 μ M Ba^{2+} . As shown in Figure 1C, this current was not affected by the application of cyto-D.

Optical Mapping of Action Potential Durations

Figure 2A shows optical action potentials from a subset of the pixels across the left ventricle of a Langendorff-perfused rat heart. These data were recorded in the presence of 3 μ M cyto-D to reduce motion artifacts. Except in areas close to the edge of the preparation, the signal was of very good quality. There are no appreciable signs of remaining motion artifact. These data were processed automatically in the manner described in 'Materials and Methods' section to yield maps of APD_{80} across the entire preparation as shown in Figure 2B. A gradient of APD_{80} such that APDs were longer at the base and shorter near the apex was generally observed, in agreement with previous results in mouse³⁶ and guinea pig.³⁷

Effects of Di-4-ANEPPS and Cyto-D

Figure 3 shows the effects of the dye di-4-ANEPPS (1 μ M) and the motion blocker cyto-D (3 μ M) on the electrogram of the Langendorff-perfused rat heart. As we have reported previously,²⁷ di-4-ANEPPS prolonged the PQ interval significantly, but did not significantly affect QRS or QT_{100} interval. Cyto-D had no significant effect on PQ or QRS interval, but caused a significant prolongation (24%) of the QT_{100} interval.

APD Shortening due to $I_{K,ATP}$ Activation

Action potential shortening in response to the application of the K_{ATP} channel opener P-1075 (2 μ M) was monitored using optical mapping in eight Langendorff-perfused rat hearts. Figure 4 shows the results of these measurements. Average APD_{80} shortened from 63.4 ± 2.5 msec under control conditions to 35.0 ± 1.5 msec in the presence of 2 μ M P-1075. Subsequent application of the sulfonyleurea (K_{ATP} channel blocker) HMR 1098 (10 μ M) caused the action potential to lengthen again to an average of 59.2 ± 1.8 msec, demonstrating that the observed action potential shortening was due to the opening of K_{ATP} channels. Conduction velocity, assessed by measuring the time elapsed from activation of 10–90% of

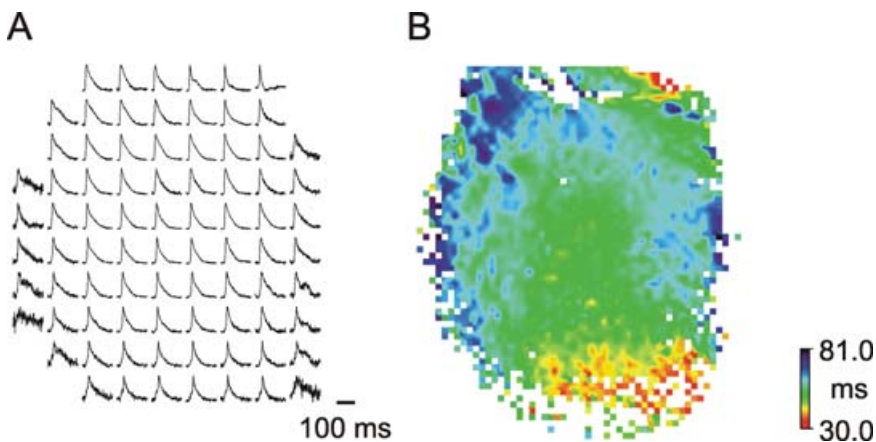
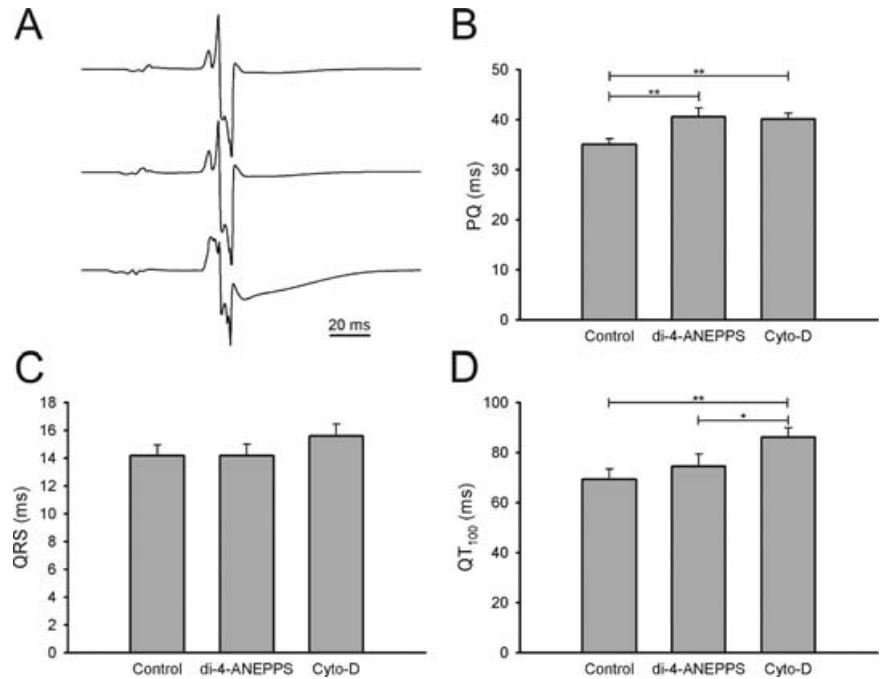


Figure 2. Optical mapping of ventricular action potential durations in a Langendorff-perfused rat heart. A: Optical action potentials from individual pixels (every sixth pixel shown) across the preparation. B: Color map showing the distribution of APD_{80} across the preparation.

Figure 3. Effects of di-4-ANEPPS and cyto-D (cyto-D) on the electrogram of the Langendorff-perfused rat heart. A: Electrograms (lead II) recorded during control conditions (top), after staining with 1 μ M di-4-ANEPPS (middle), and after adding 3 μ M cyto-D (bottom). B: Average PQ intervals ($n = 9$) lengthened significantly in response to staining with di-4-ANEPPS. C: Average QRS intervals ($n = 9$) did not change significantly in response to either di-4-ANEPPS or cyto-D. D: Average QT₁₀₀ interval ($n = 8$) lengthened significantly in response to 3 μ M cyto-D.

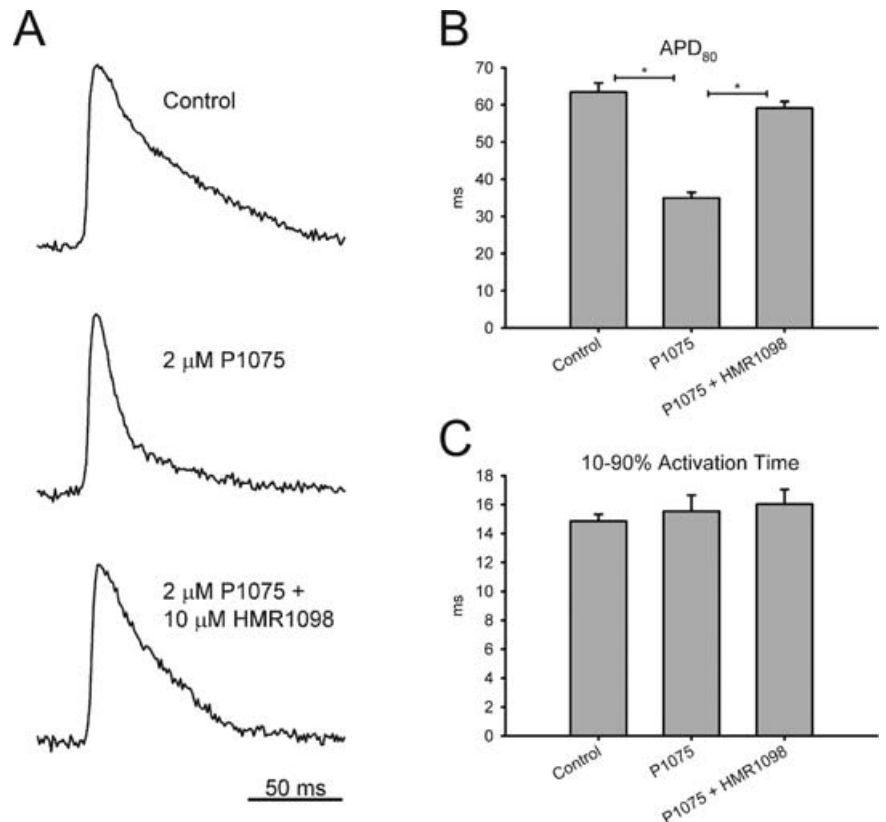


the field of view, was not significantly affected by P-1075 or HMR 1098 as shown in Figure 4C.

Three-lead surface electrograms were recorded from four of the hearts above for comparison to the optical results. Figure 5 shows a summary of the results from these measurements. Activation of $I_{K,ATP}$ current using 2 μ M P-1075 had no significant effect on either the PQ or the QRS in-

terval, consistent with the observation that P-1075 had no effect on conduction velocity in the optical recordings. However, in agreement with the observation that 2 μ M P-1075 shortens APD₈₀ in the optical recordings, the QT₁₀₀ interval shortened in response to P-1075 application from 89.8 ± 2.2 msec to 68.9 ± 3.3 msec. After application of 10 μ M HMR 1098, the QT₁₀₀ interval lengthened again to 95.0 ± 2.4 msec,

Figure 4. Optical recording of the effects of $I_{K,ATP}$ activation in response to 2 μ M P-1075. A: Typical optical action potential records from one pixel. The APD shortened in response to P-1075, and this effect was almost completely reversed by the application of the K_{ATP} channel blocker HMR 1098 (10 μ M). B: Summary data for action potential duration ($n = 8$ hearts). C: Summary data for ventricular activation time (10–90%, $n = 8$ hearts), indicating that conduction velocity was not significantly affected following $I_{K,ATP}$ activation.



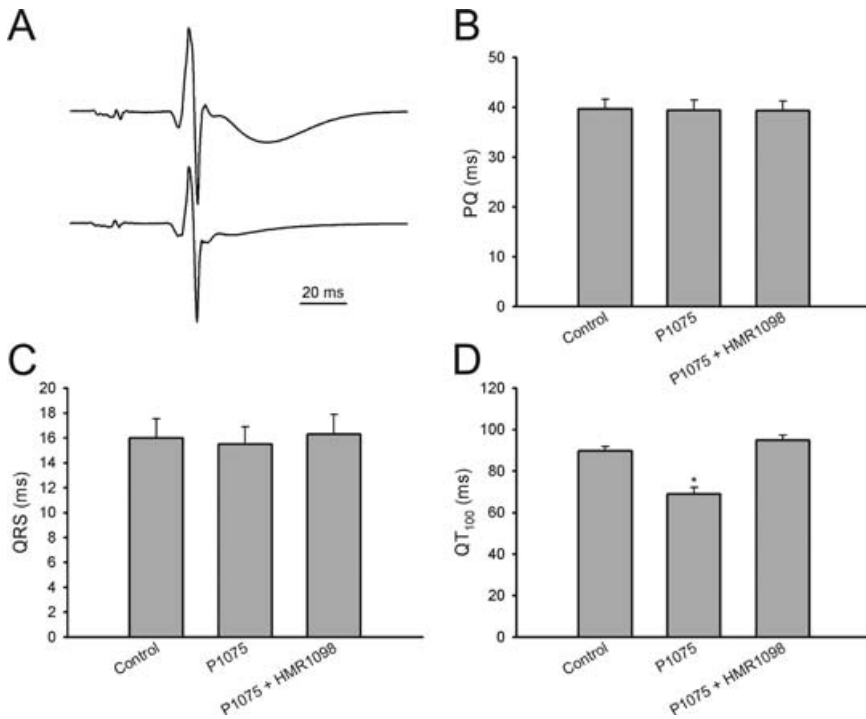


Figure 5. Effects of $I_{K,ATP}$ activation (2 μ M P-1075) on the electrogram of the Langendorff-perfused rat heart. A: Typical electrograms (lead II) recorded under control conditions (top) and after the application of P-1075 (bottom), showing shortening of the QT interval in response to P-1075. B: Average PQ interval ($n = 4$ hearts) was not affected by P-1075. C: Average QRS interval ($n = 4$ hearts) was not significantly affected by P-1075. D: Average QT₁₀₀ interval shortened significantly in response to P-1075. This effect was reversed by the application of 10 μ M HMR 1098.

demonstrating that the QT₁₀₀ shortening was due to the opening of K_{ATP} channels.

Electrophysiological Changes Due to Elevated [K⁺]_o

The electrophysiological effects of elevated extracellular [K⁺] ([K⁺]_o = 12 mM) were evaluated using optical mapping in seven Langendorff-perfused rat hearts. Figure 6 shows a summary of these results. Elevated [K⁺]_o did not have a

significant effect on APD₈₀. However, as expected, 12 mM [K⁺]_o caused a substantial slowing of conduction velocity, increasing the time for activation of 10–90% of the field of view from 16.0 ± 0.8 msec to 28.4 ± 2.4 msec. The increased [K⁺]_o also caused a significant increase in the rate of final repolarization, presumably due to the effects on the inwardly rectifying K⁺ current, I_{K1}. The average time for repolarization of the action potential from the 30% level

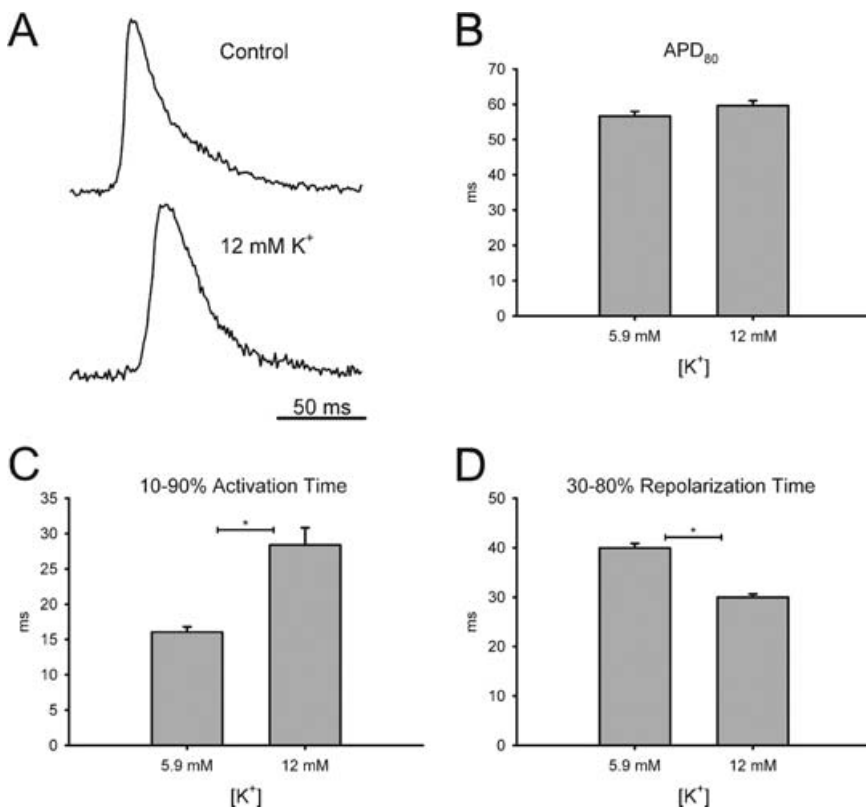
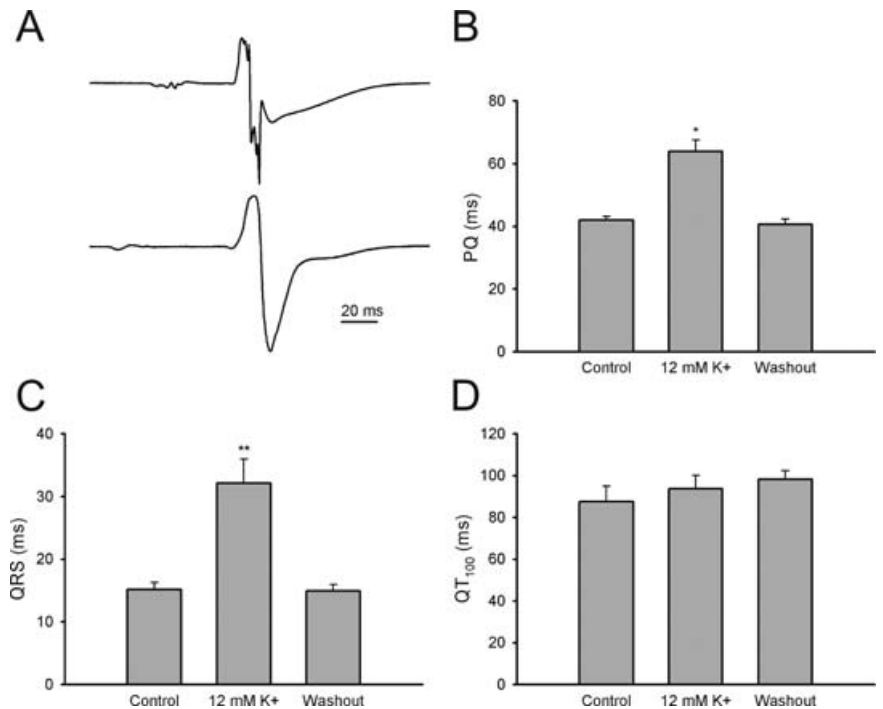


Figure 6. Optical recording of the effects of elevated K⁺ concentration (12 mM) in the perfusate. A: Typical optical action potentials from one pixel, showing delayed activation, reduced rate of rise, and increased rate of repolarization. B: Summary data for APD₈₀. Average APD₈₀ remained constant after increasing the [K⁺] in the perfusate. C: Summary data for ventricular activation time (10–90%), indicating that ventricular conduction velocity slowed significantly. D: Summary data for average time to repolarize from the 30% to the 80% level of repolarization. Note that the rate of repolarization of the action potential was significantly more rapid in 12 mM [K⁺].

Figure 7. Effects of elevated K^+ concentration (12 mM) in the perfusate on the electrogram of the Langendorff-perfused rat hearts. A: Typical electrograms (lead II) recorded under control conditions ($[K^+] = 5.9 \text{ mM}$, top) and in elevated $[K^+]$ (12 mM, bottom). The PQ and QRS intervals both lengthen as a result of conduction slowing in the higher $[K^+]$. B: Average PQ interval ($n = 5$ hearts) increased significantly in elevated $[K^+]$. C: Average QRS interval ($n = 5$ hearts) lengthened significantly in elevated $[K^+]$. D: Average QT_{100} interval ($n = 5$ hearts) did not change significantly in response to elevated $[K^+]$.



to the 80% level of repolarization was reduced from 39.9 ± 1.0 msec under control conditions ($5.9 \text{ mM } [K^+]_o$) to 30.0 ± 0.6 msec in $12 \text{ mM } [K^+]_o$. Thus, the fact that the APD_{80} remained unchanged (Fig. 6B) is the result of two opposite effects: (1) the reduced rate of rise tends to prolong the action potential, and (2) the increased rate of repolarization tends to shorten the action potential.

Three-lead surface electrograms were also recorded from five of the hearts above to study the effects of elevated $[K^+]_o$ on the electrogram, and to compare to the observations from the optical recordings. The results of these recordings are summarized in Figure 7. Elevated $[K^+]_o$ resulted in a substantial broadening of the QRS complex, consistent with the conduction slowing observed in the optical recordings (Fig. 7A). Raising $[K^+]_o$ from 5.9 mM to 12 mM lengthened the PQ interval from 41.9 ± 1.2 msec to 63.9 ± 3.7 msec, and the QRS interval from 15.2 ± 1.1 msec to 32.1 ± 3.9 msec. In agreement with the observation that APD_{80} is unaffected by elevated $[K^+]_o$ in the optical measurements, the QT_{100} interval of the electrogram was also unaffected. However, as in the case of the optical recordings, the depolarization phase (QRS interval) is lengthened whereas the repolarization phase (T wave) is shortened.

Electrophysiological Changes Due to Acidosis

The effects of acidosis (pH 6.5 in the perfusate) on the electrophysiological properties of the Langendorff-perfused rat heart were evaluated in four preparations. Figure 8 shows a summary of these results. Acidosis caused a statistically significant ($P = 0.02$, Student's *t*-test) prolongation of APD_{80} from 57.2 ± 1.5 msec at normal pH (7.4) to 67.8 ± 1.3 msec. The time from activation of 10–90% of the field of view increased somewhat from an average of 16.6 ± 0.8 msec under control conditions to 18.9 ± 1.4 msec in acidotic conditions. However, this result failed to reach statistical significance at the 0.05 level ($P = 0.06$, Student's *t*-test).

Three-lead surface electrograms were recorded from the same four Langendorff-perfused rat hearts mentioned in the previous paragraph and PQ, QRS, and QT_{100} intervals were measured. Figure 9 is a summary of these observations. Acidosis (pH 6.5) caused a significant lengthening of the PQ interval from 39.4 ± 1.0 msec at pH 7.4 to 47.1 ± 2.6 ms at pH 6.5, as well as a significant lengthening of the QRS interval from 14.2 ± 0.9 ms to 17.4 ± 0.5 msec. Consistent with the observation that APD_{80} in the optical recordings lengthened due to acidosis, the QT_{100} interval also lengthened from 97.4 ± 5.0 msec to 121.7 ± 8.7 msec.

Discussion

Cyto-D Effects on Key K^+ Currents

Cyto-D is a commonly used pharmacological tool for investigating the role of the cytoskeleton in the function of ion channels and signaling pathways.¹³ Cyto-D prevents polymerization of actin filaments, and may also sever actin filaments by binding to interior sites. A recent review by Calaghan et al.¹³ suggests that the negative inotropic effect of cyto-D is due to interaction with sarcomeric actin, rather than any effects on the cytoskeleton. However, since cyto-D also affects the cytoskeletal actin filaments, it is reasonable to expect side effects on ion channels.

Effects on $I_{K,ATP}$

Given the importance of activation of $I_{K,ATP}$ in the context of ischemia, we studied the effects of cyto-D on currents carried by the K_{ATP} channel in rat ventricular myocytes using the whole-cell configuration of the patch clamp technique. Our results show that the application of $3 \mu\text{M}$ cyto-D to isolated rat ventricular myocytes produces a significant increase in the amplitude of the $I_{K,ATP}$ current activated by $2 \mu\text{M}$ P-1075. This effect is likely due to the actions of cyto-D on the cytoskeleton. Previous studies have demonstrated that disruption of the cytoskeleton by cyto-D can interfere

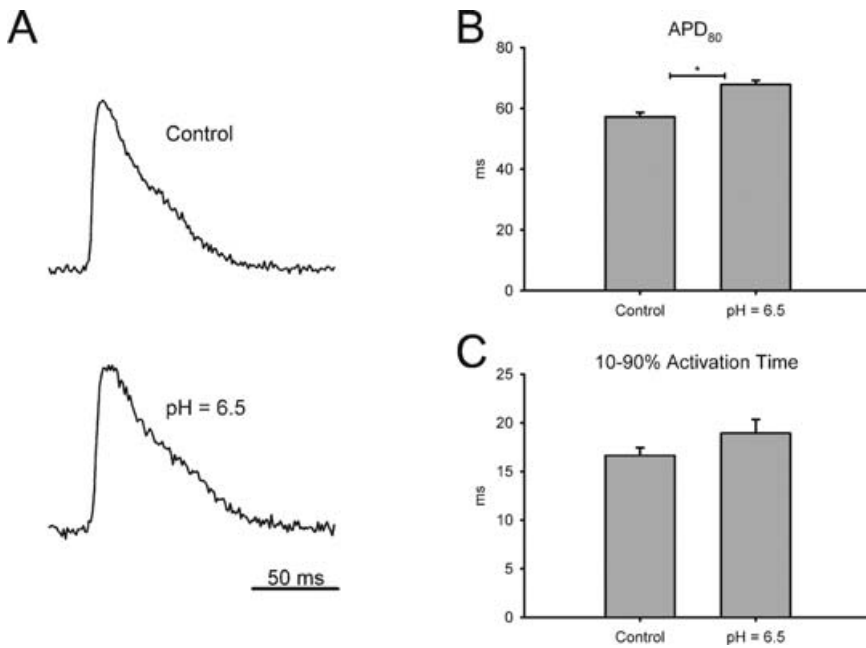


Figure 8. Optical recording of the effects of acidosis (pH = 6.5 in the perfusate) on the rat ventricular action potential. A: Optical action potentials from one pixel. B: Summary data for APD₈₀. APD₈₀ increased significantly in response to acidosis. C: Summary data for ventricular activation time (10–90%). There is a possible trend for conduction slowing in response to acidosis. However, this result did not reach statistical significance.

with the function of the sarcolemmal K_{ATP} channel.^{14–17} Disruption of the cytoskeleton has been shown to enhance K_{ATP} channel activity¹⁵ in excised patches from guinea pig ventricular myocytes, and to impair sulfonylurea inhibition of K_{ATP} channel^{16,17} activity. Both the inhibitory sulfonylurea drugs and K_{ATP} channel openers (such as P-1075) target the sulfonylurea receptor (SUR) subunit of the K_{ATP} channel.³⁸ It is therefore reasonable to expect that cyto-D will affect the efficacy of K_{ATP} channel openers as well as the sulfonylurea inhibitors. Our data support this supposition. Our data do not show the previously reported reduction in the efficacy of the K_{ATP} blocker.^{16,17} However, the difference in recording methods (whole cell vs excised patch), means of activation of

the K_{ATP} current (P-1075 vs exposure to low [ATP]), and the choice of K_{ATP} blocker (HMR 1098 vs glyburide or tolbutamide) may all have contributed to this discrepancy. Nevertheless, our observations are consistent with the hypothesis that disruption of the cytoskeleton can alter regulation of the K_{ATP} channel by the SUR subunit. Our results also demonstrate that the concentration of cyto-D required for suppression of motion artifacts in rat ventricle (3 μM²¹) is sufficient for these effects to occur.

Effects on I_{K1}

The inwardly rectifying K⁺ current, I_{K1}, is important in determining the resting potential and subthreshold electrical

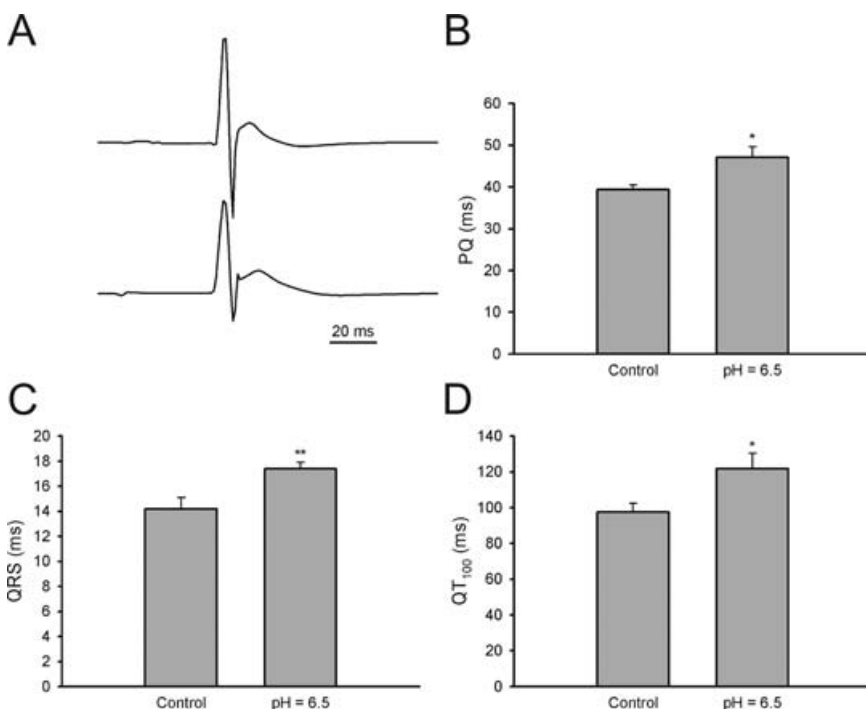


Figure 9. Effects of acidosis (pH = 6.5) on the electrogram recorded from Langendorff-perfused rat hearts. A: Typical electrograms (lead II) recorded under control conditions (pH = 7.4, top) and in response to acidosis (pH = 6.5, bottom). Lengthening of the PQ, QRS, and QT intervals is evident under acidotic conditions. B: Average PQ interval (n = 4 hearts) increased significantly in response to acidosis. C: Average QRS interval (n = 4 hearts) lengthened significantly in response to acidosis, indicating that ventricular conduction velocity slowed under these conditions. D: Average QT₁₀₀ interval (n = 4 hearts) lengthened significantly in response to acidosis.

properties of the myocyte, and thus in determining conduction velocity of the myocardium.³⁹ Data in the literature suggest that the cytoskeleton may play an important role in controlling the rectification of the K^+ channels underlying I_{K1} .¹³ We therefore evaluated the effects of cyto-D on the I_{K1} current under our recording conditions in isolated rat ventricular myocytes. Our results show that this current was unaffected by 3 μ M cyto-D. Alterations of the subthreshold electrical properties of ventricular myocytes, therefore, do not appear to be a concern under our recording conditions.

Cyto-D Effects on the Action Potential

Cyto-D prolongs the QT_{100} interval of the surface electrogram recorded from Langendorff-perfused rat hearts by 24%. We therefore assume that cyto-D prolongs the rat ventricular APD to a comparable extent. This effect on APD is consistent with previous observations in mouse ventricle,¹⁰ which showed a substantial prolongation of the action potential in response to the application of cyto-D. A likely reason for this is that cyto-D suppresses one or more of the repolarizing K^+ currents in the rat (and mouse) ventricle. The transient outward current I_{to} is the primary repolarizing current in the rat ventricle,⁴⁰ and hence this K^+ current is the most likely candidate. However, effects on other ionic currents cannot be ruled out. We have not measured cyto-D effects on currents other than $I_{K,ATP}$ and I_{K1} in the whole-cell patch clamp configuration. However, our observations are not consistent with previous observations in isolated myocytes,²³ in which cyto-D effects on I_{to} and the APD were only observed in hypertrophied myocytes.

Effects of Di-4-ANEPPS

Consistent with our previous observations,²⁷ perfusion of di-4-ANEPPS prolonged the PQ interval of the surface electrogram of Langendorff-perfused rat hearts. These recordings were carried out in 2 mM $[Ca^{2+}]$, an experimental condition that we have previously reported attenuates the prolongation of the PQ interval compared to recordings in lower $[Ca^{2+}]$. No significant effects of di-4-ANEPPS on the QRS duration or QT_{100} interval were observed. These findings suggest that the effects of di-4-ANEPPS are limited to a slight slowing of AV conduction.

Measurement of Components of the Acute Ischemic Response

Opening of K_{ATP} Channels

Opening of K_{ATP} channels has been shown to occur early in acute ischemia in response to inhibition of cell metabolism.⁴¹ As shown by the mathematical modeling studies of Shaw and Rudy,^{42,43} this is expected to result in a significant shortening of the action potential without appreciably affecting conduction velocity. Shortening of APD in response to ischemia has also been demonstrated in several studies using optical mapping in species other than the rat.^{2-4,7} Most of these studies used either BDM as a motion blocker, or no motion blocker,³ although the recent study of Liu et al. used cyto-D in rabbit hearts. Because of the possibility that cyto-D might interfere with the regulation of $I_{K,ATP}$, it was important to determine whether $I_{K,ATP}$ functions normally under our recording conditions. To focus on the effects of K_{ATP} channel opening, and to allow the possibility of reversing

the effect using a K_{ATP} channel blocker, we chose to activate $I_{K,ATP}$ using a well-characterized channel opener (P-1075) rather than by creating ischemic conditions.

APD was assessed both from the optical recordings and indirectly from the QT_{100} interval of the surface electrogram. Our results show that activation of $I_{K,ATP}$ results in the expected shortening of the APD and QT_{100} and that this effect can be reversed using HMR 1098 to block $I_{K,ATP}$. Rat ventricular K_{ATP} channels therefore appear to be regulated normally under our experimental conditions. This result is important for future studies using this method and these recording conditions, as there is some controversy in the literature regarding whether $I_{K,ATP}$ is activated in acute ischemia in the Langendorff-perfused rat heart.⁴⁴ However, our data from single isolated myocytes described above suggest that the amount of $I_{K,ATP}$ activated in response to acute ischemia under our recording conditions may be enhanced by the presence of cyto-D. We must therefore acknowledge the possibility that the regulation of K_{ATP} channels under our experimental conditions may be quantitatively altered.

Conduction velocity was assessed both in terms of the 10–90% activation time of the optical recordings, and in terms of QRS duration and PQ interval of the surface electrogram. All measures of conduction velocity were unaffected by the activation of $I_{K,ATP}$ under our recording conditions, as predicted by modeling studies.⁴²

Accumulation of Extracellular K^+

It is well known that a sustained rise in extracellular $[K^+]$ is a prominent component of the response to acute ischemia.⁴⁵⁻⁴⁷ Modeling studies,^{39,42} as well as experimental measurements,⁴⁷ show that elevated extracellular $[K^+]$ results in slowing of conduction velocity. We have previously demonstrated this classical response in Langendorff-perfused rat hearts in the absence of cyto-D.²⁷ Due to the possibility that disruption of the cytoskeleton by cyto-D might alter the properties of the inwardly rectifying K^+ current, I_{K1} , it was deemed necessary to verify this response under the current recording conditions (in the presence of cyto-D).

Conduction velocity was again assessed both in terms of the 10–90% activation time of the optical recording and in terms of the QRS (and PQ) interval of the surface electrogram. Our results show that increasing the $[K^+]$ in the perfusate to 12 mM causes a substantial slowing of conduction velocity as assessed by each of these methods. As expected, there was little change in APD in response to elevated perfusate $[K^+]$. However, the repolarization time of the action potential (measured from 30% to 80% repolarization) shortened significantly. This illustrates the complexity when using APD as a measure to assess increases in repolarizing currents in ischemia (be they due to activation of $I_{K,ATP}$ or increased outward I_{K1}): The increase in action potential rise time in response to depolarization of the resting potential may (partially) offset the decrease in repolarization time caused by an increase in $I_{K,ATP}$ and/or I_{K1} . In the context of ischemia, where opening of K_{ATP} channels and accumulation of extracellular K^+ occur simultaneously, it may therefore be more accurate to use the repolarization time as a measure of the contributions of increases in repolarizing currents. A similar ambiguity may apply to the QT_{100} interval in our surface electrogram recordings, which remained approximately the same before and after increasing perfusate $[K^+]$.

Farkas et al. provide a more detailed discussion of this phenomenon in the context of the Langendorff-perfused rat heart electrogram.⁴⁸

Acidosis

Experimental observations by Kagiya et al.,⁴⁷ as well as computational studies by Shaw and Rudy,⁴² show that acidosis in the perfusate can slow conduction velocity. This is primarily due to a reduction in the amplitude of the Na⁺ current, I_{Na}. However, for the moderate reductions in pH in this study, this effect is smaller than the effect of accumulation of extracellular [K⁺]. We created acidosis by reducing perfusate pH to 6.5⁴⁷ and measured APD and conduction velocity. This level of acidosis produced a small, but statistically significant increase in APD. This illustrates another potential difficulty in assessing the effects of acute ischemia from action potential and/or surface electrogram measurements: Different components of the ischemic response may produce opposite effects on the repolarization of the action potential (cf. the observations of Verkerk et al. in rabbit and human ventricular myocytes⁴¹). Conduction velocity, assessed in terms of QRS and PQ intervals, slowed by a small but statistically significant amount, in agreement with the observations of Kagiya et al.⁴⁷ The corresponding increase in 10–90% activation time in the optical recordings failed to reach statistical significance.

Conclusion

We have studied the electrophysiological responses to known components of acute ischemia in Langendorff-perfused rat hearts using optical mapping and surface electrograms. In addition, we have evaluated the effects of the motion blocker cyto-D in this preparation. Our results demonstrate the significant effects of the known primary components of the electrophysiological response to acute ischemia under these recording conditions, and also show that optical and electrical measurements are in agreement. In principle, therefore, the method outlined can be considered feasible for studies in which ischemia is induced, for example, by ligating a coronary artery.

However, our results raise two concerns regarding the use of cyto-D as a motion blocker. First, disruption of the cytoskeleton caused by cyto-D may lead to enhanced activity of K_{ATP} channels. We can therefore not rule out the possibility that the amount of I_{K,ATP} current activated in response to ischemia under these conditions may be larger than it would be in the absence of cyto-D. Shortening of the APD in response to ischemia may therefore be enhanced in this experimental preparation. Second, it is clear from our surface electrogram measurements (QT₁₀₀ interval) that addition of cyto-D to the perfusate produces a substantial APD prolongation. The baseline electrophysiology, even prior to ischemia, is therefore altered under these recording conditions. The dynamics of any arrhythmias that occur as a result of ischemia may therefore be altered as well.^{49,50} In summary, our results not only provide essential baseline information for interpreting recordings in the presence of cyto-D in the Langendorff-perfused rat heart, but also highlight the need for nonpharmacological approaches to suppression of motion artifact in voltage-sensitive dye recordings in the heart.^{51,52}

Acknowledgments: The authors acknowledge excellent technical assistance provided by Ms. Colleen Kondo.

References

1. Efimov IR, Nikolski VP, Salama G: Optical imaging of the heart. *Circ Res* 2004;95:21-33.
2. Cheng Y, Mowrey KA, Nikolski V, Tchou PJ, Efimov IR: Mechanisms of shock-induced arrhythmogenesis during acute global ischemia. *Am J Physiol Heart Circ Physiol* 2002;282:H2141-H2151.
3. Efimov IR, Huang DT, Rendt JM, Salama G: Optical mapping of repolarization and refractoriness from intact hearts. *Circulation* 1994;90:1469-1480.
4. Holley LK, Knisley SB: Transmembrane potentials during high voltage shocks in ischemic cardiac tissue. *Pacing Clin Electrophysiol* 1997;20:146-152.
5. Knisley SB, Holley LK: Characterization of shock-induced action potential extension during acute regional ischemia in rabbit hearts. *J Cardiovasc Electrophysiol* 1995;6:775-785.
6. Salama G, Kanai A, Huang D, Efimov IR, Girouard SD, Rosenbaum DS: Hypoxia and hypothermia enhance spatial heterogeneities of repolarization in guinea pig hearts: Analysis of spatial autocorrelation of optically recorded action potential durations. *J Cardiovasc Electrophysiol* 1998;9:164-183.
7. Liu YB, Pak HN, Lamp ST, Okuyama Y, Hayashi H, Wu TJ, Weiss JN, Chen PS, Lin SF: Coexistence of two types of ventricular fibrillation during acute regional ischemia in rabbit ventricle. *J Cardiovasc Electrophysiol* 2004;15:1433-1440.
8. Zaitsev AV, Guha PK, Sarmast F, Kolli A, Berenfeld O, Pertsov AM, de G Jr, Coronel R, Jalife J: Wavebreak formation during ventricular fibrillation in the isolated, regionally ischemic pig heart. *Circ Res* 2003;92:546-553.
9. Liu Y, Cabo C, Salomonsz R, Delmar M, Davidenko J, Jalife J: Effects of diacetyl monoxime on the electrical properties of sheep and guinea pig ventricular muscle. *Cardiovasc Res* 1993;27:1991-1997.
10. Baker LC, Wolk R, Choi BR, Watkins S, Plan P, Shah A, Salama G: Effects of mechanical uncouplers, diacetyl monoxime, and cytochalasin-D on the electrophysiology of perfused mouse hearts. *Am J Physiol Heart Circ Physiol* 2004;287:H1771-H1779.
11. Cheng Y, Li L, Nikolski V, Wallick DW, Efimov IR: Shock-induced arrhythmogenesis is enhanced by 2,3-butanedione monoxime compared with cytochalasin D. *Am J Physiol Heart Circ Physiol* 2004;286:H310-H318.
12. Boban M, Stowe DF, Kampine JP, Goldberg AH, Bosnjak ZJ: Effects of 2,3-butanedione monoxime in isolated hearts: Protection during reperfusion after global ischemia. *J Thorac Cardiovasc Surg* 1993;105:532-540.
13. Calaghan SC, Le Guennec JY, White E: Cytoskeletal modulation of electrical and mechanical activity in cardiac myocytes. *Prog Biophys Mol Biol* 2004;84:29-59.
14. Furukawa T, Yamane T, Terai T, Katayama Y, Hiraoka M: Functional linkage of the cardiac ATP-sensitive K⁺ channel to the actin cytoskeleton. *Pflügers Arch* 1996;431:504-512.
15. Terzic A, Kurachi Y: Actin microfilament disrupters enhance K(ATP) channel opening in patches from guinea-pig cardiomyocytes. *J Physiol* 1996;492(Pt 2):395-404.
16. Brady PA, Alekseev AE, Aleksandrova LA, Gomez LA, Terzic A: A disrupter of actin microfilaments impairs sulfonyleurea-inhibitory gating of cardiac KATP channels. *Am J Physiol* 1996;271:H2710-H2716.
17. Yokoshiki H, Katsube Y, Sunugawa M, Seki T, Sperelakis N: Disruption of actin cytoskeleton attenuates sulfonyleurea inhibition of cardiac ATP-sensitive K⁺ channels. *Pflügers Arch* 1997;434:203-205.
18. Wu J, Bierman M, Rubart M, Zipes DP: Cytochalasin D as excitation-contraction uncoupler for optically mapping action potentials in wedges of ventricular myocardium. *J Cardiovasc Electrophysiol* 1998;9:1336-1347.
19. Bierman M, Rubart M, Moreno A, Wu J, Josiah-Durant A, Zipes DP: Differential effects of cytochalasin D and 2,3 butanedione monoxime on isometric twitch force and transmembrane action potential in isolated ventricular muscle: Implications from optical measurements of cardiac repolarization. *J Cardiovasc Electrophysiol* 1998;9:1348-1357.
20. Lee MH, Lin SF, Ohara T, Omichi C, Okuyama Y, Chudin E, Garfinkel A, Weiss JN, Karagueuzian HS, Chen PS: Effects of diacetyl monoxime and cytochalasin D on ventricular fibrillation in swine right ventricles. *Am J Physiol* 2001;280:H2689-H2696.

21. Kettlewell S, Walker NL, Cobbe SM, Burton FL, Smith GL: The electrophysiological and mechanical effects of 2,3-butane-dione monoxime and cytochalasin-D in the Langendorff perfused rabbit heart. *Exp Physiol* 2004;89:163-172.
22. Jalife J, Morley GE, Tallini NY, Vaidya D: A fungal metabolite that eliminates motion artifacts. *J Cardiovasc Electrophysiol* 1998;9:1358-1362.
23. Yang X, Salas PJ, Pham TV, Wasserlauf BJ, Smets MJ, Myerburg RJ, Gelband H, Hoffman BF, Bassett AL: Cytoskeletal actin microfilaments and the transient outward potassium current in hypertrophied rat ventriculocytes. *J Physiol* 2002;541:411-421.
24. Curtis MJ, Macleod BA, Walker MJ: Models for the study of arrhythmias in myocardial ischaemia and infarction: The use of the rat. *J Mol Cell Cardiol* 1987;19:399-419.
25. Curtis MJ: Characterisation, utilisation and clinical relevance of isolated perfused heart models of ischaemia-induced ventricular fibrillation. *Cardiovasc Res* 1998;39:194-215.
26. Abbott A: The renaissance rat. *Nature* 2004;428:464-466.
27. Nygren A, Kondo C, Clark RB, Giles WR: Voltage-sensitive dye mapping in Langendorff-perfused rat hearts. *Am J Physiol Heart Circ Physiol* 2003;284:H892-H902.
28. Carmeliet E: Cardiac ionic currents and acute ischemia: From channels to arrhythmias. *Physiol Rev* 1999;79:917-1017.
29. Bouchard RA, Clark RB, Giles WR: Role of sodium-calcium exchange in activation of contraction in rat ventricle. *J Physiol* 1993;472:391-413.
30. Light P, Shimoni Y, Harbison S, Giles W, French RJ: Hypothyroidism decreases the ATP sensitivity of KATP channels from rat heart. *J Memb Biol* 1998;162:217-223.
31. Bouchard R, Clark RB, Juhasz AE, Giles WR: Changes in extracellular K⁺ concentration modulate contractility of rat and rabbit cardiac myocytes via the inward rectifier K⁺ current IK1. *J Physiol* 2004;556:773-790.
32. Nygren A, Clark RB, Belke DD, Kondo C, Giles WR, Witkowski FX: Voltage-sensitive dye mapping of activation and conduction in adult mouse hearts. *Ann Biomed Eng* 2000;28:958-967.
33. Liu Y, Ren G, O'Rourke B, Marban E, Seharaseyon J: Pharmacological comparison of native mitochondrial K(ATP) channels with molecularly defined surface K(ATP) channels. *Mol Pharmacol* 2001;59:225-230.
34. Gögelein H, Englert HC, Kotzan A, Hack R, Lehr K-H, Seiz W, Becker RHA, Sultan E, Schölkens BA, Busch AE: HMR 1098: An inhibitor of cardiac ATP-sensitive potassium channels. *Cardiovasc Drug Rev* 2000;18:157-174.
35. Manning Fox JE, Kanji HD, French RJ, Light PE: Cardiospecificity of the sulfonylurea HMR 1098: Studies on native and recombinant cardiac and pancreatic K(ATP) channels. *Br J Pharmacol* 2002;135:480-488.
36. Baker LC, London B, Choi BR, Koren G, Salama G: Enhanced dispersion of repolarization and refractoriness in transgenic mouse hearts promotes reentrant ventricular tachycardia. *Circ Res* 2000;86:396-407.
37. Kanai A, Salama G: Optical mapping reveals that repolarization spreads anisotropically and is guided by fiber orientation in guinea pig hearts. *Circ Res* 1995;77:784-802.
38. Gribble FM, Reimann F: Pharmacological modulation of K(ATP) channels. *Biochem Soc Trans* 2002;30:333-339.
39. Nygren A, Giles WR: Mathematical simulation of slowing of cardiac conduction velocity by elevated extracellular [K⁺] in a human atrial strand. *Ann Biomed Eng* 2000;28:951-957.
40. Pandit SV, Clark RB, Giles WR, Demir SS: A mathematical model of action potential heterogeneity in adult rat left ventricular myocytes. *Biophys J* 2001;81:3029-3051.
41. Verkerk AO, Veldkamp MW, van Ginneken AC, Bouman LN: Biphasic response of action potential duration to metabolic inhibition in rabbit and human ventricular myocytes: Role of transient outward current and ATP-regulated potassium current. *J Mol Cell Cardiol* 1996;28:2443-2456.
42. Shaw RM, Rudy Y: Electrophysiologic effects of acute myocardial ischemia: A mechanistic investigation of action potential conduction and conduction failure. *Circ Res* 1997;80:124-138.
43. Shaw RM, Rudy Y: Electrophysiologic effects of acute myocardial ischemia: A theoretical study of altered cell excitability and action potential duration. *Cardiovasc Res* 1997;35:256-272.
44. Workman AJ, MacKenzie I, Northover BJ: Do KATP channels open as a prominent and early feature during ischaemia in the Langendorff-perfused rat heart? *Basic Res Cardiol* 2000;95:250-260.
45. Kléber AG: Resting membrane potential, extracellular potassium activity, and intracellular sodium activity during acute global ischemia in isolated perfused guinea pig hearts. *Circ Res* 1983;52:442-450.
46. Weiss J, Shine KI: Extracellular K⁺ accumulation during myocardial ischemia in isolated rabbit heart. *Am J Physiol* 1982;242:H619-H628.
47. Kagiya Y, Hill JL, Gettes LS: Interaction of acidosis and increased extracellular potassium on action potential characteristics and conduction in guinea pig ventricular muscle. *Circ Res* 1982;51:614-623.
48. Farkas A, Curtis MJ: Does QT widening in the Langendorff-perfused rat heart represent the effect of repolarization delay or conduction slowing? *J Cardiovasc Pharmacol* 2003;42:612-621.
49. Hayashi H, Miyauchi Y, Chou CC, Karagueuzian HS, Chen PS, Lin SF: Effects of cytochalasin D on electrical restitution and the dynamics of ventricular fibrillation in isolated rabbit heart. *J Cardiovasc Electrophysiol* 2003;14:1077-1084.
50. Qin H, Kay MW, Chattipakorn N, Redden DT, Ideker RE, Rogers JM: Effects of heart isolation, voltage-sensitive dye, and electromechanical uncoupling agents on ventricular fibrillation. *Am J Physiol Heart Circ Physiol* 2003;284:H1818-H1826.
51. Knisley SB, Justice RK, Kong W, Johnson PL: Ratiometry of transmembrane voltage-sensitive fluorescent dye emission in hearts. *Am J Physiol Heart Circ Physiol* 2000;279:H1421-H1433.
52. Rohr S, Kucera JP: Optical recording system based on a fiber optic image conduit: Assessment of microscopic activation patterns in cardiac tissue. *Biophys J* 1998;75:1062-1075.